ORIGINAL ARTICLE

Explosion mitigation by metal grid with water curtain

T. Schunck[1] · M. Bastide[1] · D. Eckenfels[1] · J. F. Legendre[1]

Abstract

This paper examines blast mitigation based on geometric means, namely a perforated plate or a chain mail, with or without a water film cover. This method may be used for the protection of structures, and its effectiveness and limitations were assessed. First, a shock tube was used to visualize the interaction of a blast wave profile with a metallic grid or with a metallic grid covered by a layer of water. Secondly, free-field air blast experiments were performed in order to evaluate the protection system under real conditions. Three types of grids were tested. The first was a metallic plate having small round holes, the second had large round holes, and the third had square holes. A chain mail made of steel rings was also tested. The porosity of the grids ranged from 48 to 69%. In case of a collision between a shock wave and a grid, it was observed that one part of the incident shock wave was reflected by the plate. The remaining part was transmitted through the plate. The overpressure and the impulse downstream from the grid were reduced, and the reduction increased when the porosity decreased. When a film of water covered the grid, it was observed that the water film disintegrated into droplets long after the passage of the blast wave. Filling the holes with water enhanced the overpressure and impulse reduction as it contributed to the reflection of the shock wave.

Keywords Blast · Mitigation · Grid · Water curtain

1 Introduction

The protection of people and structures against the effects of blast waves is of utmost importance since the number of terrorist attacks on civilian and military infrastructure continues to rise all over the world. Different protective façade elements have been proposed and studied, and among them metal ring meshes in combination with a down-streaming water curtain [1]. These are modern architectural design elements, which can be used inside or outside buildings.

The description of the interaction of a shock wave with grid-like obstacles started in the 1950s [2]. Grids or perforated plates modify the flow field by introducing new shock waves, regions of vortices, and considerable turbulence in

which the energy of the incident shock wave can be dissipated. In 1977, Kingery et al. [3] assessed the attenuation of a shock wave passing through a perforated plate in a shock tube with a shock wave having a blast profile. They investigated the effect of peak overpressure and of holes of different sizes by using several areas vented at different percentages. The following phenomenon was observed: when the percentage of openings was increased, the attenuation decreased. In addition, the value of the overpressure used had only a small effect on the percentage of attenuation. More recently, Britan et al. [4] also described the shock wave interaction with a perforated plate in a shock tube. When a shock wave collides with a perforated plate, a part of the incident shock wave is reflected by the plate and the other part is transmitted, generating a non-steady flow behind the plate. The flow located immediately behind the grid is highly unsteady and non-uniform. It becomes steady and uniform further downstream. The transmitted wave is mostly attenuated in the region where the flow is highly turbulent. According to the authors, the shock attenuation depends on the porosity of the plate, on the shape of the open spaces in the plate, and on the spatial distribution of these open spaces. In 2006, Britan et al. [5] investigated the full cycle of reflections that resulted in the

Communicated by D. Frost.

✉ T. Schunck
therese.schunck@isl.eu

[1] French-German Research Institute of Saint-Louis (ISL), 5 rue du Général Cassagnou, 68301 Saint-Louis, France

air gap between the plate and the end wall of the shock tube as well as the pressure effects on the end of the shock tube. They assessed the effect of barrier porosity on shock wave attenuation and particularly on the rate of pressure increase acting on the end wall. Their results showed that the strength of the incident shock wave, the barrier porosity, and the distance between the barrier and the end wall were the major factors influencing the pressure attenuation. The geometry of the holes had practically no influence.

The usage of water barriers for mitigating the damage from blast waves generated by an explosion has been described in the literature [6–10]. Water can be used in various physical forms. This includes bulk water [6,8] and water spray or mist [9,10]. This technique is considered "passive" as the kinetic energy of the explosion is used to disperse the water or to break the water container and disperse the water. It was investigated for the use in mines but also for protecting ammunition storages and civilian facilities. In most of these studies, the detonating charge was surrounded by a large amount of water and, in this case, pressure reductions were large. If the water was placed at a certain distance, the attenuation was much lower [8]. The literature on the quantitative study on mitigation efficiency of water walls is very limited. Recently, Chen et al. [11] have investigated the influence of wall thickness, water/charge distance, and also the water wall height. A charge of 0.2 kg TNT was detonated on the ground in front of a water wall that comprised a steel frame containing plastic bags filled with water. The overpressure was measured at different distances behind the water wall. It has been shown that the wall thickness had little effect on the blast wave mitigation but that the wall height as well as the distance between the water and the charge affected the overpressure reduction. For a distance range of 40–50 cm behind the water wall, the overpressure reduction was about 77–79%. A smaller water–charge distance and a higher water wall led to a more effective mitigation of the peak incident overpressure. According to the authors, the mitigation stemmed from the fact that the blast wave was obstructed, reflected, and diffracted by the water wall, and the mitigation mechanism was similar to that of rigid wall.

These two methods could be combined wisely to protect building façades or walls. Gebbeken et al. [1] tested such a solution made of a stainless steel ring mesh in combination with a flowing water layer. Two explosion tests with a spherical charge of 3.9 kg PETN were conducted. The charges were located 5 m in front of the ring mesh with or without a water cover, and several pressure gauges were placed on the shock wave path. The reflected overpressure was also measured on a wall located 5 m behind the ring mesh. Three tests without grid were also carried out. For the ring mesh alone, they described an initial side-on overpressure reduction of approximately 17% at 50 cm behind the grid and of around 1–6% at 1.5–2.5 m behind the grid. When the ring mesh

was covered by water, the initial side-on overpressure was reduced by 56% close behind the ring mesh and by 20% farther away behind the mesh. As regards the positive impulse, the ring mesh itself caused no reduction but, adding the water curtain, a reduction of about 17–31% was obtained behind the mesh. Consequently, this blast mitigation method appears promising but lacks sufficient data to confirm validation.

In this paper, this blast mitigation solution is explored in more detail, and a perforated plate or a chain mail with or without a water film cover serves as an obstacle. This solution is investigated in order to verify its effectiveness and limitations. First, a shock tube was used to visualize the interaction of a blast wave profile with a metallic grid or with a metallic grid covered by a water layer. Secondly, free-field air blast experiments were performed in order to evaluate the protection system under real conditions. Three types of grids were tested. The first was a metallic plate having small round holes, the second had large round holes, and the third had square holes. A chain mail made of steel rings was also tested.

2 Materials and methods

2.1 Shock tube

A transonic shock tube was used, and modifications were carried out in order to generate a shock wave with a blast profile. A Friedlander-type wave (pressure jump followed by progressive decay) is obtained at a specific location in the tube. The shock tube comprised four sections: the driver section at high pressure (400 mm in diameter, 500 mm long), the driven section at atmospheric pressure (400 mm in diameter, 6970 mm long), the measurement section, which was rectangular (235 mm × 235 mm) with 220-mm-long viewing glass windows, and the extension section after the measurement section (rectangular and 1120 mm long), see Fig. 1. The measurement section is connected to the driven tube by means of a "cookie-cutter". The extension section prevented shock reflections at the end of the tube from coming backward and disturbing the pressure signals during the effective measurement time. Before the test, the driver tube and the driven tube are separated by a Mylar diaphragm so that the high-pressure gas filling can be carried out in the driver tube. When the desired pressure level in the driver tube is reached, the diaphragm is perforated by a piercing device controlled by an electromagnetic valve.

The experiments were conducted under the following conditions: for a pressure of 1.5 bar in the driver section and 1 bar in the driven section, a shock wave with a Mach number of 1.15 and an incident overpressure of 0.3 bar is generated. One PCB pressure gauge (Piezotronics 113A21 model) located 54.5 mm upstream from the grid and two PCB pres-

sure gauges (Piezotronics 113A21 model) located 35 and 214.5 mm downstream from the grid recorded the over-pressure profile. High-speed video recordings were obtained for each experiment. Differential interferometry was used to visualize the shock wave propagation and its interaction with the grid or with the grid covered by a water film. A high-speed Photron SA-Z camera was used to record videos with a frame rate of 20,000 fps at the full resolution of 1024×1024 pixels. The exposure time of each frame was 158 ns.

For all experiments, the light source was a 100-W halogen horizontal filament lamp. The goal of the experimental device is to entirely illuminate the measurement chamber windows with parallel light. The visualization set-up was a differential or shearing interferometer [12] in a standard Z-configuration with two parabolic mirrors of focal length 1500 mm and diameter 300 mm. The used Wollaston prisms had a prism angle of 2°, and the imaging lens had a focal length of 135 mm. The system was set up to provide vertical fringes and therefore shows density gradients in horizontal (flow) direction. The optical set-up is presented in Fig. 2. A close-up of the experimental set-up in the measurement section of the shock tube is presented in Fig. 3. It consists of a metal grid and a cylindrical water tank (22.5 cm length and 3 cm diameter). The water tank is fixed on the top of the grid and is split along its length (17.5 cm), thereby allowing for the runoff of the water on the entire surface of the grid. Water is supplied to the tank via a tube and a pump. The water flow was about 757 mL/min. The grid has the same size as the section of the measurement chamber.

Three types of metal grids were tested: the first was a metallic plate having small round holes, the second had large round holes, and the third had square holes (Fig. 4). The characteristics of the grids are given in Table 1.

2.2 Free field

In free field, explosion tests were conducted with homogenous spheres of 1 kg composition B. The charges were raised by 25 cm, and they were ignited by a high voltage cap and a booster charge of 44 g of Semtex. The charge was positioned 3 m from the grid, and two PCB sensors (PCB137A23) were used to evaluate the effect of the grid or of the grid covered by the water layer on the blast wave profile. The Mach number of the blast wave at this position was 1.4. The first and the second gauges were placed 25 cm and 3 m behind the grid, respectively. The sensors were positioned at a height of 30 cm. The three types of metal grids (Fig. 4, Table 1) were tested, and also a chain mail made of steel rings (Fig. 5). The characteristics of the chain mail are given in Table 1. The grid size was 1 m $\times$ 1 m, and concrete blocks placed on the left and on the right of the grid were used to mount the grid (Fig. 6). Each of them had the following dimensions:

length 50 cm, height 1 m, and width 1 m. A parallelepipedic water tank was fixed on the top of the grid allowing for the runoff of the water on the entire surface of the grid. Water is supplied to the tank via a tube.

3 Results

3.1 Shock tube

3.1.1 Imaging

Figure 7 shows a sequence of differential interferograms of the shock wave propagation through a metallic plate having square holes. When passing through the holes ($t = 4.55$ ms), the shock wave split into several shock waves ($t = 4.6$ ms), one for each hole, and these shock waves recombined a few centimetres downstream from the grid. At $t = 4.95$ ms, the complex structure of the shock wave resulting from the several shock waves was still visible behind the grid. The remaining shock wave, which did not pass through the grid, was reflected by the grid. This led to the pattern at the back of the grid. The reflected shock wave and the part that has passed through the grid had approximately the same velocity as the distance covered in a given time by the two shock waves was about equal. In this case, the wave pattern was symmetrical about the grid. The figure resulting from the interaction of the shock wave with the grid was similar for the grids having round holes. It was noticeable that a region of turbulence formed behind the grid long after the passage of the shock wave. This was particularly noticed for the grids having round holes (Fig. 8). At $t = 4.75$ ms, these regions began to form behind the grid, and at $t = 5$ ms, they were still observable. They were still very marked for a duration of 0.55 ms and over a distance of several centimetres.

Figure 9 shows the shock wave propagation through a metallic plate having large round holes covered by water. When passing through the holes, the shock wave generated numerous wavelets that recombined further downstream. The water film obstructing the holes broke into droplets long after the passage of the shock front. The shock wave impacted the grid at 4.6 ms, and the break-up started approximately at $t = 4.9$ ms. The water may be sucked by the air flow behind the shock front. These droplets formed jets at each grid hole. This phenomenon was observed for all grid types. The water mist generated by the break-up of the water film persisted for a long period of time. It was still visible after 15 ms and over a distance of about ten centimetres.

3.1.2 Pressure and impulse profile

Three reference tests were conducted with no grid placed in the shock tube, and three tests were run for each type of grid
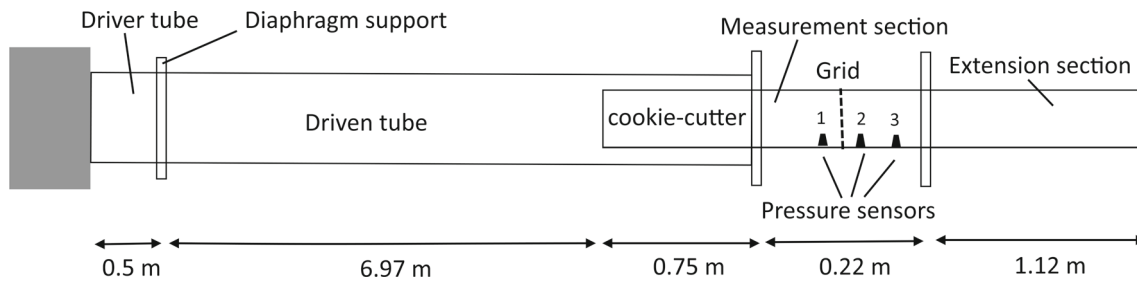
Fig. 1 Schematic sketch of the ISL shock tube with all dimensions in m. The position of the grid in the measurement section is indicated. Sensor 1: pressure gauge located 54.5 mm upstream from the grid. Sen-sor 2: pressure gauge located 35 mm downstream from the grid. Sensor 3: pressure gauge located 214.5 mm downstream from the grid

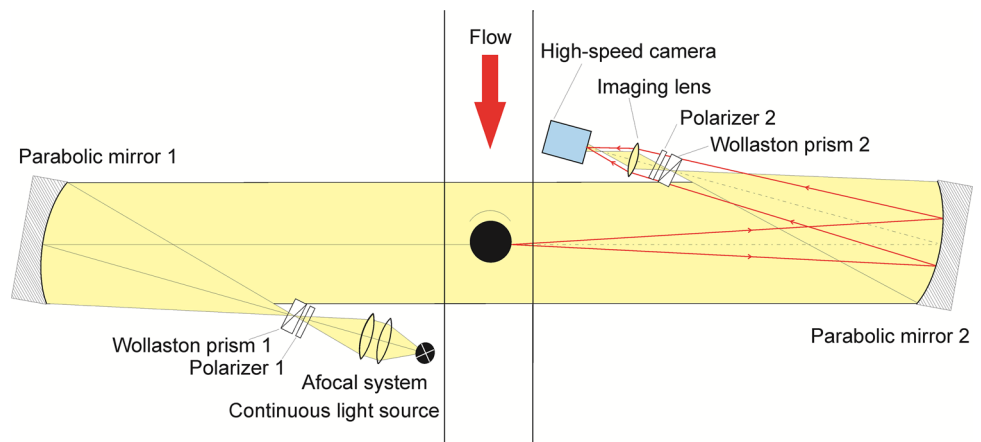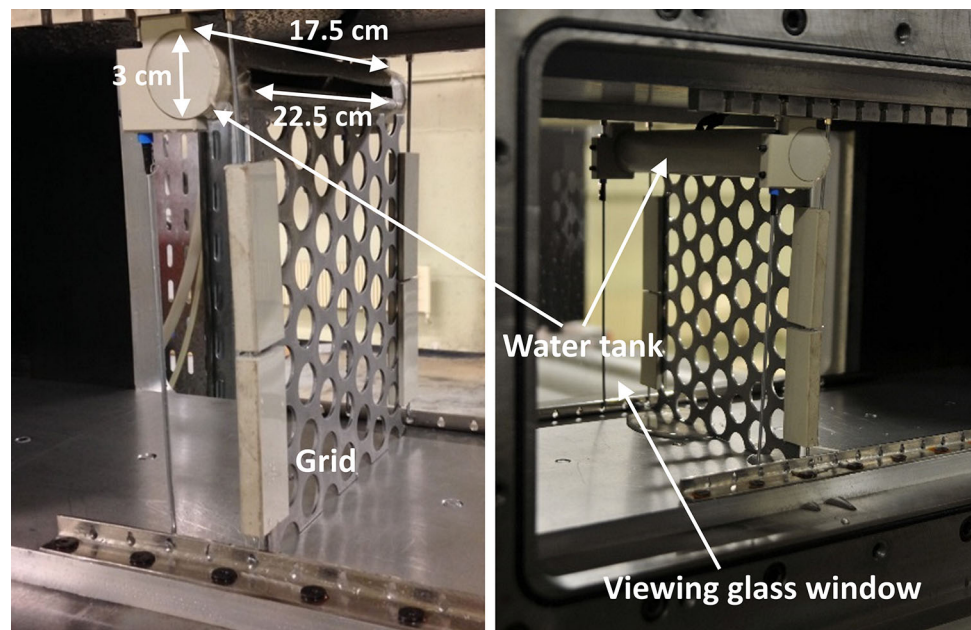**Fig. 2** Optical set-up for differential interferometry

Fig. 3 Close-up of the experimental set-up in the measurement section of the shock tube. The grid and its mounting system and the water tank allowing the water runoff on the grid in the measurement chamber are shown

with and without water cover. The overpressure versus time was recorded by the sensor located 35 mm upstream from the grid and with the two PCB pressure gauges located 35 and 214.5 mm downstream from the grid, respectively. The impulse, which is the pressure signal integrated over time, was computed as a function of time. The initial overpressure, the maximum impulse, and the arrival time for all the tests are given in Table 2. The difference between the value obtained upstream from the grid and the value obtained downstream from the grid is also given.
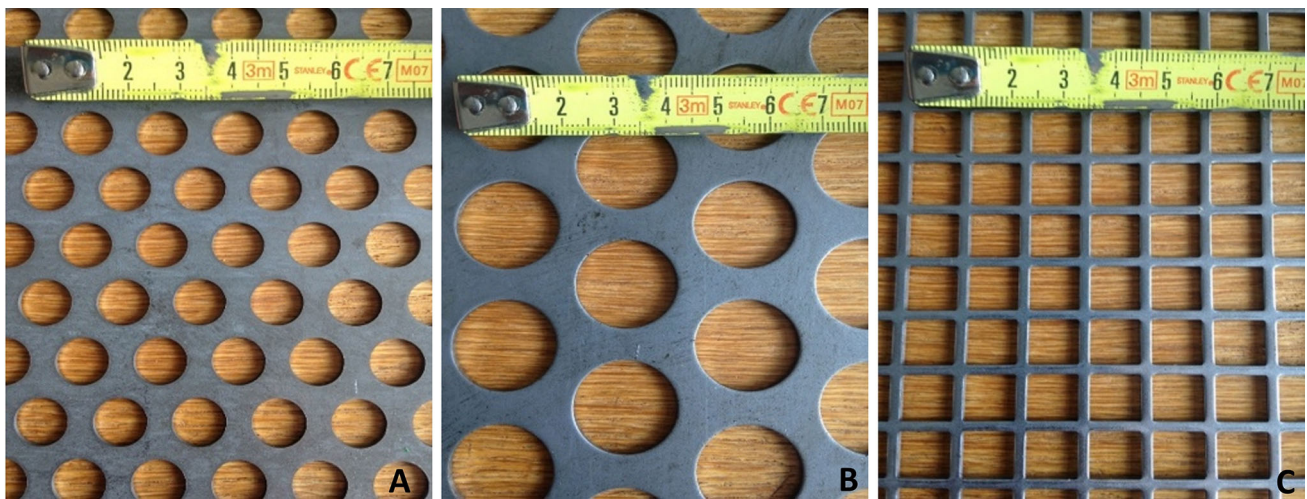
Fig. 4 Metal grids. **a** Small round holes (10 mm dia., distance between holes 14 mm); porosity 48% and plate thickness 1.5 mm. **b** Large round holes (20 mm dia., distance between holes 27 mm); porosity 49.8% and plate thickness 2 mm. **c** Square holes (10 mm × 10 mm, distance between holes 12 mm); porosity 69.4% and plate thickness 1.5 mm

Table 1 Characteristics of the grids and of the chain mail

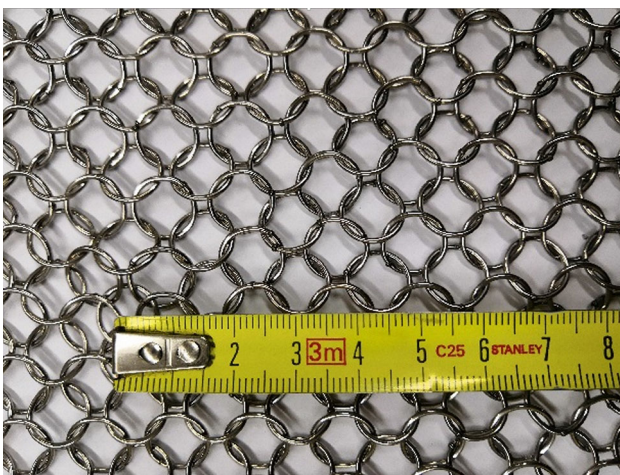|	Small round holes	Large round holes	Square holes	Chain mail
Porosity (%)	48	49.8	69.4	63
Hole size (mm)	10	20	10	12
Thickness (mm)	1.5	2	1.5	–
Distance between the holes (mm)	14	27	12	1.1 (ring thickness)

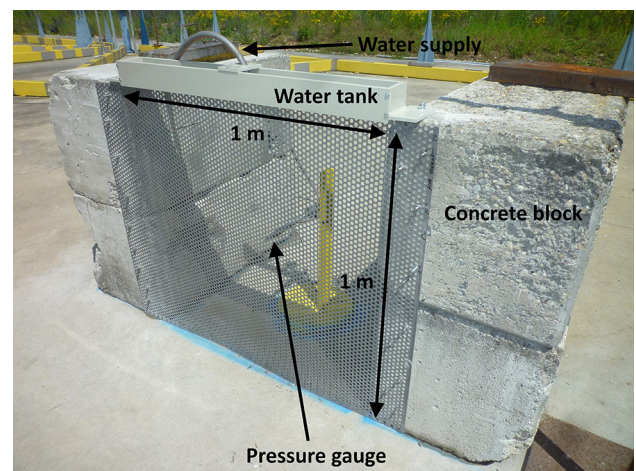**Fig. 5** Chain mail: porosity 63%, hole size 12 mm, and ring thickness 1.1 mm

Fig. 6 Free-field experimental set-up showing the concrete blocks used for grid fixing, the grid, the gauge behind the grid, and the water tank

For the reference tests, it was observed that the pressure profile as well as the impulse was very reproducible for the three sensors. Moreover, except for the time delay, the pressure and impulse levels are equivalent for the three gauges (Table 2).

For the grid having large round holes, the overpressure downstream from the grid appeared to have decreased by about 10–20%. The impulse was also reduced by the presence of the grid (of the order of 10–15%) (Table 2). The same results were obtained with the grid having small round holes (Table 2). The grid having square holes had almost no impact
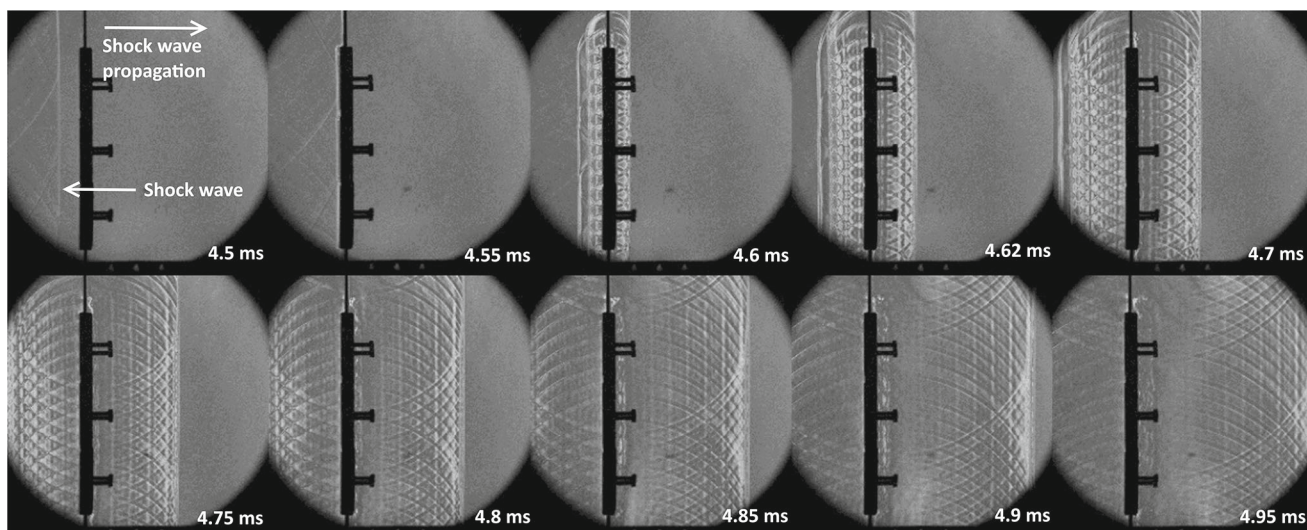
Fig. 7 Frames from a time-resolved differential interferometry visualization, showing the shock wave propagation through a metallic plate having square holes (50 μs between shown frames)
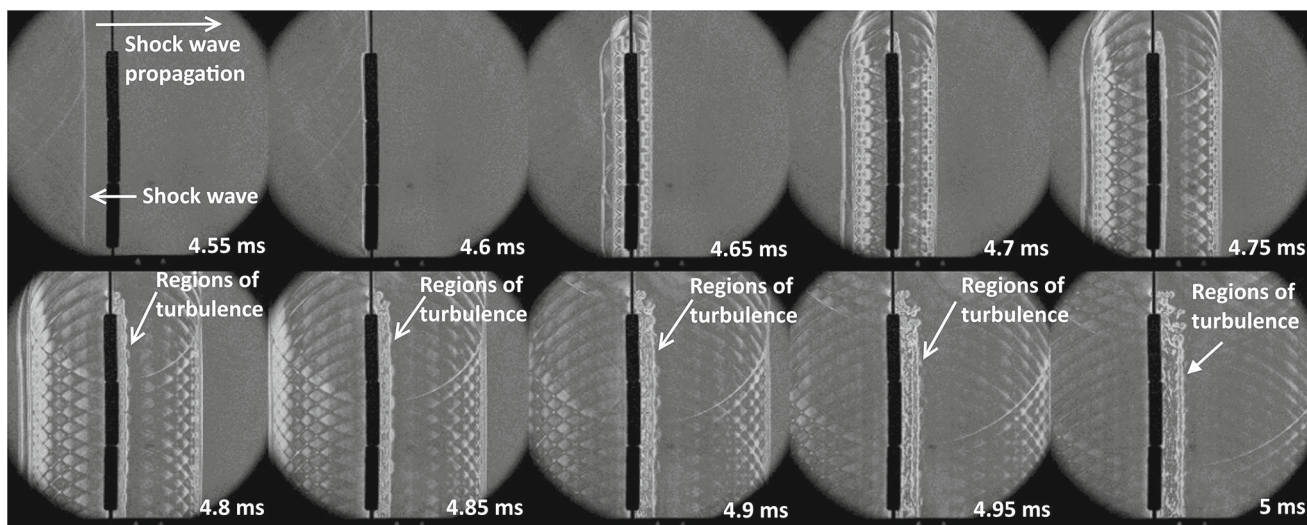

Fig. 8 Frames from a time-resolved differential interferometry visualization, showing the shock wave propagation through a metallic plate having small round holes (50 μs between shown frames). The regions of turbulence behind the grid are outlined

on the overpressure and on the impulse (Table 2). Figure 10 presents the overpressure versus time obtained with the three sensors for the grid having large round holes for the three experiments. The reflection of the shock wave on the grid is visible on the sensor located upstream from the grid at about 0.0058 s. This was also clearly observed for the grid having small round holes but not for the grid having square holes. The shock overpressure values corresponding to the reflected shock wave obtained with the sensor located upstream from the grid are given in Table 2. The values were similar for the grids having round holes, but they were very low for the grid having square holes.

For the grids having round holes and covered by a water film, the overpressure and the impulse decreased downstream

from the grid. The reduction was slightly increased when they were covered by a layer of water. When the grid having square holes was covered by water, the overpressure downstream from the grid was clearly reduced (of the order of 15–25%), and the impulse was also clearly decreased by about 10–15%. The reflection of the shock wave off the grids having round holes and covered by water was also visible on the sensor located upstream from the grid, and the reflected overpressure values were a little bit higher compared to the values obtained with the grids alone. The reflection of the shock wave on the grid having square holes covered by a water layer was still not obvious (Table 2).
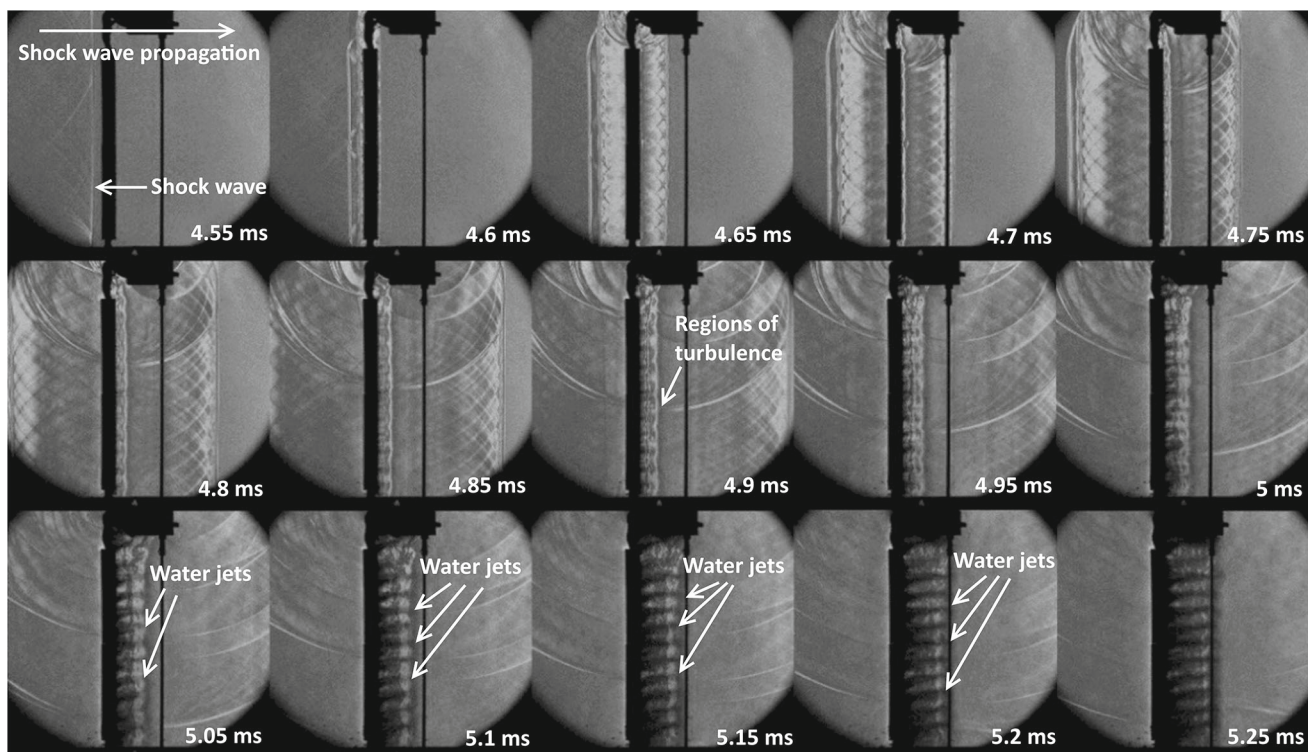
Fig. 9 Frames from a time-resolved differential interferometry visualization, showing the shock wave propagation through a metallic plate having large round holes covered by water (50 μs between shown frames). The regions of turbulence and the water jets forming behind the grid are outlined

3.2 Free field

3.2.1 Overpressure

Three reference tests were conducted with no grid and three tests with each type of grid with and without water cover. Table 3 presents the initial overpressure obtained with the two sensors placed downstream from the grid for all experiments and also the difference with respect to the mean values obtained in the reference tests. Twenty-five centimetres downstream from the grid, the initial overpressure was reduced for the grids having round holes (of the order of 17–25%). The grid having square holes had also an effect but less consistent, and the chain mail had almost no impact. The initial overpressure 3 m downstream from the grid was reduced for the grids having round holes by about 25–30%. The grid having square holes and the chain mail had a smaller effect.

When the grids were covered by a water layer, the initial overpressure was reduced for all grid types. The most pronounced reduction was obtained for the grid having small round holes, from 35 to 48%. The initial overpressure 3 m downstream from the grid was also reduced for this grid type by about 20–30%.

3.2.2 Impulse

Figure 11 presents the impulse versus time obtained with the sensor placed 25 cm downstream from the grid for all experiments. The impulse was strongly reduced by the grids having round holes, by about 25–30% but to a lesser extent for the grid having square holes (10%). The chain mail had the least effect on the impulse. Impulses obtained with the sensor placed 3 m downstream from the grid are presented in Fig. 12. The effect of the grids on the impulse profiles was observable in the first part of the curves (before 0.011 s). Indeed, over this time period, the impulse was lower for the tests with grids. After 0.011 s, the tendencies of the impulse traces were difficult to analyse. A pressure gauge drift could occur, but it cannot be excluded that the grids initially attenuated the waves but that their recombination later led to a stronger wave. This behaviour is currently not fully understood and needs to be revisited. The most pronounced reduction was obtained for the grid having small round holes, and the chain mail had almost no impact. The reduction was of the order of 20–25%. Figure 13 presents the impulse versus time obtained with the sensor placed 25 cm downstream from the grid covered by water for all experiments. The impulse was reduced for all the grids covered by water. A strong attenuation was observed for grids having

Table 2 Initial overpressure recorded by the sensor located 35 mm (*P*1) upstream from the grid, and the two PCB pressure gauges located 35 (*P*2) and 214.5 mm (*P*3) downstream from the grid

	P1 (bar)	Prefl (bar)	P2 (bar)	P3 (bar)	$I1 \cdot 10^{-3}$ (bar s)	$I2 \cdot 10^{-3}$ (bar s)	$I3 \cdot 10^{-3}$ (bar s)	t1 (ms)	t2 (ms)	t3 (ms)	Δ(P1–P2) (%)	Δ(P1–P3) (%)	Δ(I1–I2) (%)	Δ(I1–I3) (%)
Ref 1	0.27	–	0.26	0.25	0.69	0.71	0.7	5.5	5.7	6.2	–4	–7	3	1
Ref 2	0.23	–	0.23	0.22	0.68	0.68	0.68	5.6	5.8	6.3	0	–4	0	0
Ref 3	0.25	–	0.25	0.24	0.67	0.67	0.67	5.3	5.8	6.3	0	–4	0	0
LRH1	0.26	0.11	0.23	0.20	0.71	0.6	0.64	5.5	5.7	6.2	–12	–23	–15	–10
LRH2	0.26	0.12	0.22	0.20	0.72	0.6	0.65	5.4	5.7	6.2	–15	–23	–17	–10
LRH3	0.25	0.12	0.23	0.20	0.73	0.61	0.65	5.5	5.7	6.2	–8	–20	–16	–11
SRH1	0.21	0.09	0.20	0.18	0.71	0.57	0.62	5.5	5.8	6.3	–5	–14	–20	–13
SRH2	0.24	0.11	0.21	0.20	0.78	0.61	0.67	5.5	5.7	6.2	–13	–17	–22	–14
SRH3														
SH1	0.24	0.05	0.23	0.21	0.68	0.64	0.65	5.5	5.7	6.2	–4	–13	–6	–4
SH2	0.19	0.03	0.19	0.18	0.58	0.56	0.56	5.6	5.8	6.3	0	–5	–3	–3
SH3	0.20	0.04	0.20	0.20	0.63	0.61	0.61	5.5	5.8	6.2	0	0	–3	–3
LRH1 w	0.26	0.15	0.20	0.24	0.76	0.57	0.62	5.5	5.7	6.2	–23	–8	–25	–18
LRH2 w	0.24	0.15	0.21	0.21	0.68	0.58	0.6	5.5	5.8	6.2	–13	–13	–15	–12
LRH3 w	0.27	0.16	0.20	0.22	0.76	0.58	0.64	5.5	5.7	6.2	–26	–19	–24	–16
SRH1 w	0.23	0.12	0.20	0.19	0.74	0.54	0.6	5.6	5.7	6.3	–13	–17	–27	–19
SRH2 w	0.22	0.09	0.20	0.19	0.77	0.53	0.59	5.5	5.7	6.2	–9	–14	–31	–23
SRH3 w	0.23	0.14		0.19	0.75		0.61	5.5		6.2		–17		–19
SH1 w	0.27	0.05	0.23	0.20	0.74	0.62	0.66	5.5	5.7	6.2	–15	–26	–16	–11
SH2 w	0.27	0.06	0.23	0.20	0.71	0.61	0.64	5.5	5.7	6.2	–15	–26	–14	–10
SH3 w	0.27	0.05	0.23	0.20	0.7	0.61	0.65	5.5	5.7	6.2	–15	–26	–13	–7

The corresponding maximum impulses (*I*1, *I*2, and *I*3) and the arrival times (*t*1, *t*2, and *t*3) are also indicated. The difference between the value obtained upstream from the grid and the value obtained downstream from the grid is given in the last four columns. *P*refl is the shock overpressure corresponding to the reflected shock wave obtained with *P*1. Ref reference test where no grid was placed in the shock tube; LRH: large round holes; SRH: small round holes; SH: square holes; w: covered by a water film. The uncertainties associated with measurements were +/−0.1 ms for times and +/−0.05 bar for pressures

Table 3 Initial overpressure recorded by the sensors located 25 cm (*P*1) and 3 m (*P*2) downstream from the grid

	*P*1 (bar)	*P*2 (bar)	*t*1 (s)	*t*2 (s)	Pressure difference with reference mean (*P*1) (%)	Pressure difference with reference mean (*P*2) (%)
Ref 1	1.22	0.34	0.0035	0.0098		
Ref 2	1.19	0.35	0.0036	0.0099		
Ref 3	1.26	0.34	0.0036	0.0099		
LRH1	1.01	0.26	0.0037	0.01	−17	−24
LRH2	1.02	0.25	0.0036	0.01	−17	−27
LRH3	1.02	0.25	0.0036	0.01	−17	−27
SRH1	0.93	0.24	0.0037	0.0103	−24	−30
SRH2	0.93	0.25	0.0037	0.0103	−24	−27
SRH3	0.92	0.25	0.0036	0.0103	−25	−27
SH1	1.17	0.28	0.0037	0.01	−4	−18
SH2	1.02	0.28	0.0037	0.01	−17	−18
SH3	0.98	0.28	0.0037	0.01	−20	−18
CM1	1.23	0.29	0.0037	0.01	1	−16
CM2	1.15	0.29	0.0037	0.0099	−6	−16
CM3	1.14	0.29	0.0036	0.01	−7	−16
LRH1 w	0.86	0.24	0.0037	0.0105	−30	−30
LRH2 w	0.87	0.24	0.0037	0.0104	−29	−30
LRH3 w	0.85	0.24	0.0037	0.0105	−31	−30
SRH1 w	0.75	0.24	0.0037	0.0103	−39	−30
SRH2 w	0.64	0.24	0.0036	0.0102	−48	−30
SRH3 w	0.8	0.24	0.0037	0.0102	−35	−30
SH1 w	0.97	0.24	0.0036	0.0102	−21	−30
SH2 w	0.99	0.24	0.0036	0.0101	−19	−30
SH3 w	1.09	0.24	0.0036	0.0103	−11	−30
CM1 w	0.89	0.27	0.0039	0.0104	−27	−21
CM2 w	0.86	0.27	0.0037	0.0103	−30	−21
CM3 w	0.76	0.28	0.0037	0.0102	−38	−18

The arrival times (*t*1 and *t*2) and the difference with the mean values obtained with the reference tests are also given. Ref: reference test with no grid; LRH: large round holes; SRH: small round holes; SH: square holes; CM: chain mail; w: covered by a water film
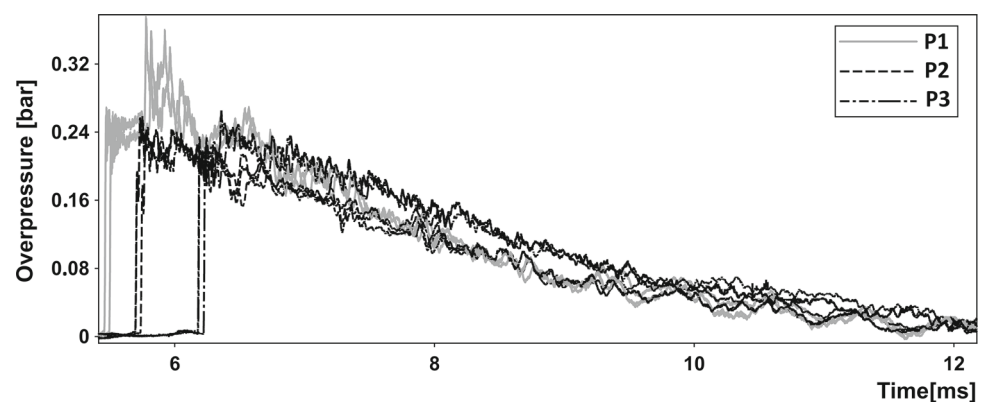
Fig. 10 Overpressure versus time obtained in the shock tube with the sensor placed 54.5 mm upstream from the grid (*P*1) and with the two sensors placed 35 and 214.5 mm downstream from the grid (*P*2 and *P*3), for the grid having large round holes. Each configuration was tested three times

Fig. 11 Impulse versus time obtained in free-field tests with the sensor placed 25 cm downstream from the grid for all tests. Reference: tests where no grid was used; LRH: large round holes; SRH: small round holes; SH: square holes; CM: chain mail
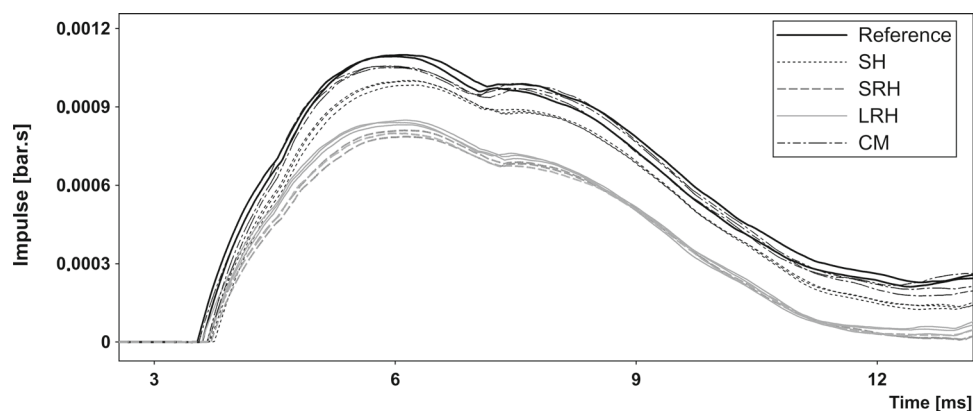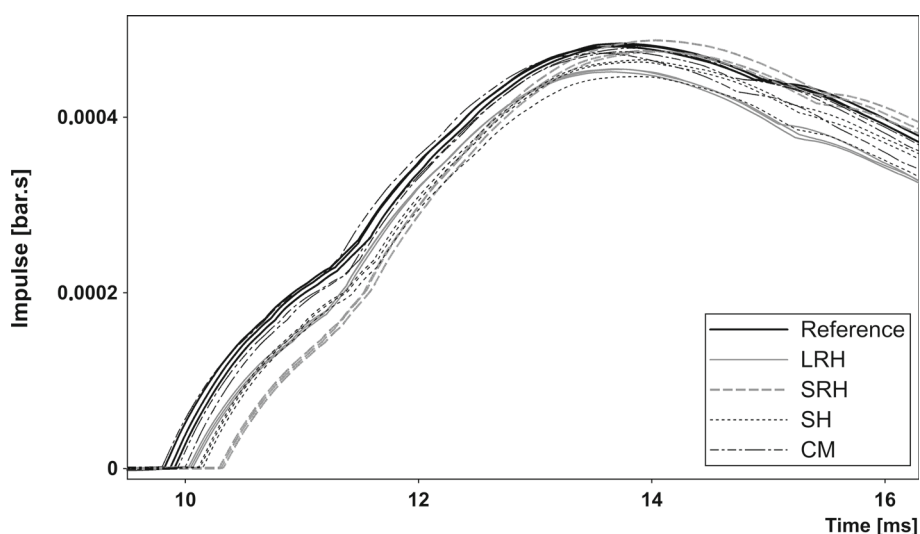
Fig. 12 Impulse versus time obtained in free-field tests with the sensor placed 3 m downstream from the grid for all tests. Reference: tests where no grid was used; LRH: large round holes; SRH: small round holes; SH: square holes; CM: chain mail

round holes, about 25–35%, and slightly less for the grid having square holes and the chain mail, about 20%. The impulse profiles obtained with the sensor placed 3 m downstream from the grid covered by water for all experiments are presented in Fig. 14. Before 0.011 s, the impulse was reduced by the presence of the grids covered by water by about 20–40%. After 0.011 s, the impulse traces for the grid having small round holes and the chain mail were greater than those of reference tests. In the same way as for the grids without water cover, this observation was difficult to explain and needs to be further investigated.

4 Discussion

The shock tube experiments have shown that when a shock wave collided with a perforated plate, a part of the incident shock wave was reflected by the plate, and the other part was transmitted through the plate. Upon colliding head-on with the grids, wave systems similar to those described in a previous study [4] occurred. When passing through the holes, the shock wave split into shocklets, one for each hole, and

they recombined further downstream. The complex structure of these shocklets was visible over a few centimetres behind the grid.

In the current tests, as expected, the overpressure and the impulse downstream from the grid were reduced, and the reduction increased when the porosity decreased. The grid having square holes had only a small impact on the overpressure and on the impulse. This was probably due to the high percentage of voids within the grid (69.4%), and consequently, the shock wave was transmitted to a larger extent. Moreover, it is important to recall that the reflection of the shock wave on the grid was not visible on the sensor located upstream from the grid having square holes. The fact that the flow presented less unsteadiness behind the grid having square holes led presumably to less energy consumption of the shock wave in this region characterized by vortices and turbulence. In the case of the two grids having round holes, while the size of the holes as well as the distance between the holes was different, the porosity was quite similar (48% and 49.8%). The effect on the overpressure and the impulse was in the same range. These grids reflected well the shock wave, as was noticed on the gauge located upstream from the
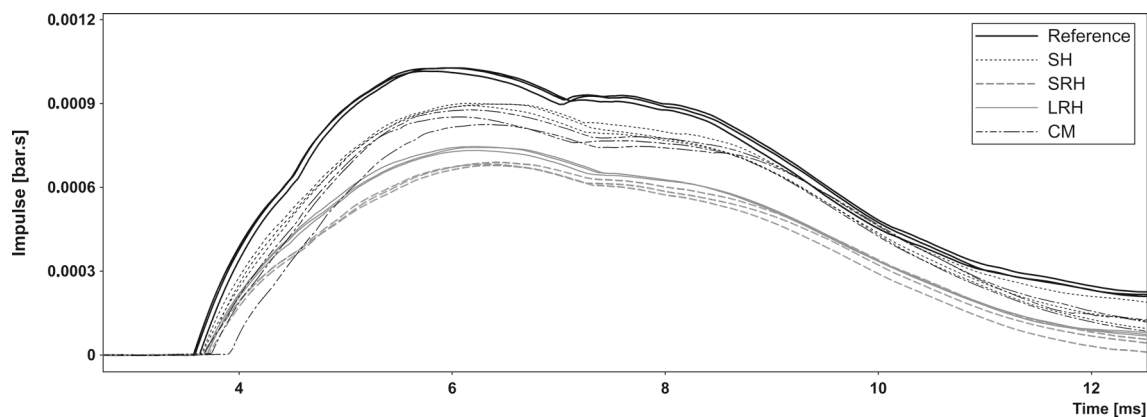
Fig. 13 Impulse versus time obtained in free-field tests with the sensor placed 25 cm downstream from the grid covered by a water film for all tests. Reference: tests where no grid was used; LRH: large round holes; SRH: small round holes; SH: square holes; CM: chain mail

grid, and strong turbulence was formed behind the grid. Thus, the shock wave attenuation increased when the grid porosity decreased. These results were in line with previously published studies [3–5,13–15]. Indeed, in these papers, it has been shown that the porosity has the main effect on the overpressure reduction. Kingery [3] assessed the effect of number of holes and hole size on shock wave attenuation for different incident peak overpressures. Porosities of 5–50% were tested, and the number and diameter of the holes were varied for each porosity value. The experimental results have shown that a perforated plate did not change appreciably its ability to attenuate shock waves when the hole size was changed. Britan et al. [4] observed that at large distances downstream of the plate, the specific shape of the perforated plate had no influence on the pressure as long as the porosity was kept at a constant value. Numerical simulations led to same results [15]. The shape of the hole could have an impact if the plates are thick and the holes bevelled. Thus, the reflection of the shock wave could be enhanced.

In free field, results with respect to shock and impulse attenuation were obtained. The less porous grids had the greatest effect on the overpressure and the impulse. The reductions were greater for the grids having round holes than for the grid having square holes and the chain mail. The attenuation of a stronger shock wave was also observed and was even greater than that obtained in the shock tube. The diffraction of a shock wave depends on its strength, and consequently, one can assume that this is the origin of the observed differences.

Regarding the perforated plate or grid thickness, one comment could be made. If the grids are thin and consequently poorly resistant to a high loading, the grids could deform and tear and some debris could impact the structure behind. The effects will be detrimental. On the contrary, if the grids are very thick, intrinsically they will be strongly resistant to the blast. Moreover, the holes could be bevelled, and therefore,
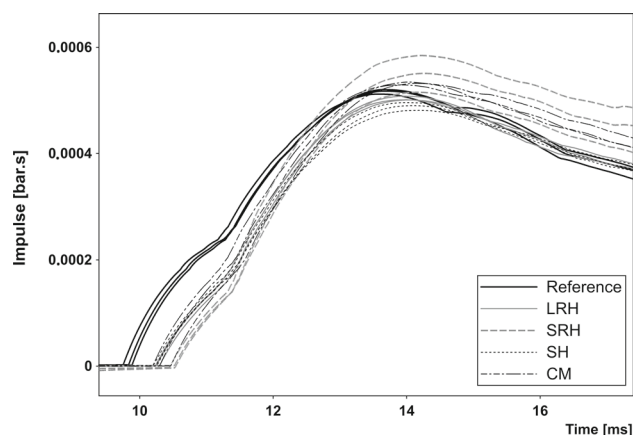

Fig. 14 Impulse versus time obtained in free-field tests with the sensor placed 3 m downstream from the grid covered by a water film for all tests. Reference: tests where no grid was used; LRH: large round holes; SRH: small round holes; SH: square holes; CM: chain mail

the blast mitigation could be improved. A three-dimensional grid could be a good option.

When a water film covered the grid, the attenuation of the shock wave downstream from the grid was increased. This trend was observed in the shock tube and in the free-field experiments. Filling the holes with water enhanced the effect of the grid on the overpressure and on the impulse. The attenuation of the shock wave behind the grid was enhanced for all grid types. While the grid having square holes and the chain mail alone were not really effective, they became truly efficient when covered with a layer of water. With the help of experiments in the shock tube, it was observed that the water film disintegrated into droplets long after the passage of the shock wave front. It is likely that the fragmentation of the water film had little effect on the attenuation as it broke long after the passage of the shock wave front. The extraction of energy from the shock front for water layer fragmentation is probably small. For the shock tube experiments, this is

confirmed by the higher reflected pressure obtained for the grid with a water cover. Indeed, a slight increase in these values was observed. The water layer contributed mostly to enhance the reflection of the shock wave. Consequently, the overpressure and the impulse reduction downstream from the grid were enhanced. According to the study [11] on blast mitigation using a water wall, the mitigation arises from the obstruction, the reflection, and the diffraction of the blast wave by the water wall, and the mitigation mechanism is comparable to that of a rigid wall. The comparison with the rigid wall proved that the mitigation effect of energy exchange with water is not the major effect and that only a small part of the blast wave energy was transformed into kinetic energy in the form of droplets.

The results obtained with the chain mail can be compared to those obtained by Gebbeken et al. [1]. These authors also mentioned that only the ring mesh itself causes a small reduction in the peak overpressure of the blast wave and no reduction in the impulse. The addition of a water curtain enhanced the attenuation of both the peak overpressure and the positive impulse. For the ring mesh alone, the results reported in [1] indicate an initial side-on overpressure reduction of approximately 17% at 50 cm behind the grid and of around 1–6% at 1.5–2.5 m behind the grid. When the ring mesh was covered by water, the initial side-on overpressure was reduced by 56% close behind the ring mesh and by 20% farther away behind the mesh. As regards the positive impulse, the ring mesh itself caused no reduction, but adding the water curtain a reduction of about 17–31% was obtained behind the mesh. Close behind the chain mail, the blast reduction achieved here was somewhat lower than the one obtained by Gebbeken et al., but farther away behind the mesh the attenuation was a little bit greater. It could be noted that they were able to evaluate the shock wave reflection by the chain mail with and without water cover, as they placed a sensor 50 cm upstream the chain mail. They observed the peak of the reflected blast wave, and they mentioned a 46.1% greater reflected peak overpressure when the ring mesh was covered by water. These authors also claimed that when the blast wave hits the ring mesh covered by water, the water layer forms a closed surface that reflects the blast wave to a greater extent. The results achieved in the present work are rather consistent with those obtained by Gebbeken et al. although their study was achieved with a greater explosive mass. One factor that can influence the results is the amount of water that flows on the chain mail. Gebbeken et al. stated that there is no known possibility to measure the thickness of the water layer. They have a notion of the total water flow, and they estimated the limits of the water thickness. It ranged from 0.25 to 5.5 mm. Unfortunately, we were not able to estimate properly the quantity of water that was present on the grid at the time the shock wave impacted it covered by water.

Therefore, it is difficult to discuss the blast wave attenuation as a function of water curtain thickness.

5 Conclusion

In this paper, we investigated the mitigation of a blast wave after its passage through a perforated plate or a chain mail with or without a water film cover. First, a shock tube was used to visualize the interaction of a blast wave profile with perforated plates or with perforated plates covered by a water film. Secondly, free-field air blast experiments were performed in order to evaluate the protection system under real conditions. Four porous barriers were tested with a porosity from 48 to 69%. It was observed that the overpressure and the impulse downstream from the grid were reduced and that the reduction increased when the porosity decreased. It is well understood that the use of a solid steel plate will not result in the best mitigation effect. In this case, the solid plate will deform or tear and may impact the structure behind and the effect will be even worse. The addition of a water layer to the grid contributed to enhance the reflection of the shock wave, and consequently, the attenuation of the shock wave downstream from the grid was increased. In the same way, the addition of a water layer to a solid steel plate will not modify its behaviour when it is subjected to a highly dynamic loading caused by an explosion.

Overall, this method seems to be of interest for protection purposes but still needs some further work and improvement. First, a method for measuring the water curtain thickness should be developed. This will allow for the study of blast mitigation in relation to this parameter. The mitigation of the shock wave may be improved if more water flows over the grid. The remaining step will be to assess the transmitted pressure on a wall placed behind this protection system and to measure the shock wave reflection by the grid using a sensor located upstream from the grid. The effect of the separation distance between the grid and the target to be protected on blast mitigation could also be investigated. Langdon et al. [16] have investigated the blast mitigation effect of perforated plates (one hole) by evaluating the plastic deformation of a target plate located behind the perforated plate. It has been shown that increasing the separation distance between the perforated plate and the target plate decreased the target plate deformation and increased the impulse at which tearing initiated.

The use of a configuration with two plates and a water film could represent one option of improvement. Indeed, it has been shown that shock wave trapping between two perforated plates enhanced the shock wave attenuation downstream from the grids [17]. This configuration will be investigated in the future.

References

1. Gebbeken, N., Rüdiger, L., Warnstedt, P.: Explosion mitigation by water mist-ring mesh with water curtain. 25th Military Aspects of Blast and Shock Conference, The Hague, Netherlands (2018)

2. Dosanjh, D.S.: Interaction of grids with traveling shock waves. NACA TN 3680, John Hopkins University (1956)

3. Kingery, C., Pearson, R., Coulter, G.: Shock wave attenuation by perforated plates with various hole sizes. USA Ballistic Research Laboratory Memorandum Report no. 2757 (1977). https://apps.dtic.mil/sti/citations/ADA041854

4. Britan, A., Karpov, A.V., Vasilev, E.I., Igra, O., Ben-Dor, G., Shapiro, E.: Experimental and numerical study of shock wave interaction with perforated plate. J. Fluid Eng. **126**, 399–409 (2004). https://doi.org/10.1115/1.1758264

5. Britan, A., Igra, O., Ben-Dor, G., Shapiro, E.: Shock wave attenuation by grids and orifice plates. Shock Waves **16**, 1–15 (2006). https://doi.org/10.1007/s00193-006-0019-0

6. Buzukov, A.A.: Decreasing the parameters of an air shock wave using an air–water curtain. Combust. Explos. Shock Waves **36**, 395–404 (2000). https://doi.org/10.1007/BF02699393

7. Pitiot, F., Chabin, P., Desailly, D.: Blast wave mitigation by water: full scale tests and numerical modelling. 29th DDESB Explosives Safety Seminar, New Orleans, USA (2000)

8. Forsen, R., Carlberg, A., Eriksson, S.: Small scale tests on mitigation effects of water in a model of the Klotz Club Installation in Alvdalen. 27th DoD Explosives Safety Seminar, Las Vegas, USA (1996)

9. Mataradze, E., Krauthammer, T., Chikhradze, N., Chagelishvili, E.: Shock energy absorber for protection of underground structure from internal explosions. 15th International Symposium on Interaction of the Effects of Munitions with Structures, Postdam, Germany (2013)

10. Schunck, T., Bastide M., Eckenfels, D., Sturtzer, M.-O., Mory, J., Legendre, J.-F.: Mitigation of blast in a water mist: effect of the detonation configuration. 25th Military Aspects of Blast and Shock Conference, The Hague, Netherlands (2018)

11. Chen, L., Zhang, L., Fang, Q., Mao, Y.-M.: Performance based investigation on the construction of anti-blast water wall. Int. J. Impact Eng. **81**, 17–33 (2015). https://doi.org/10.1016/j.ijimpeng.2015.03.003

12. Merzkirch, W.: Flow Visualization, 2nd edition. Elsevier, Amsterdam (2012)

13. Nguyen, T.-T.N., Davey, T., Proud, W.G.: Percolation of gas and attenuation of shock waves through granular beds and perforated Sheets. Proceedings of the 17th International Seminar "New Trends in Research of Energetic Materials", University of Pardubice, Czech Republic, pp. 351–358 (2014)

14. Makki, E.A.: Experimental studies on mitigating the risk of air blast loading. Open Access Dissertations, Paper 601 (2017). https://digitalcommons.uri.edu/oa_diss/601

15. Pavan Kumar, C.H.V.L.C.S., Hitesh Reddy, C., Rahul Sai, L., Dharani Kumar, K.S.S., Nagaraja, S.R.: Attenuation of shock waves using perforated plates. IOP Conf. Ser. Mater. Sci. Eng. **225**, 012059 (2017). https://doi.org/10.1088/1757-899X/225/1/012059

16. Langdon, G., Nurick, G., Du Plessis, N., Rossiter, I.: Using perforated plates as a blast wave shielding technique for application to tunnels. Appl. Mech. Mater. **82**, 467–472 (2011). https://doi.org/10.4028/www.scientific.net/AMM.82.467

17. Seeraj, S.: Shock wave interactions with porous plates. Master Degree Thesis, Faculty of Engineering, University of the Witwatersrand, Johannesburg, South Africa (2007)